ANTIOXIDANTS & REDOX SIGNALING
Volume 16, Number 5, 2012

DOI: 10.1089/ars.2011.4062

ORIGINAL RESEARCH COMMUNICATION

Coagulation Activation Is Associated with Nicotinamide Adenine Dinucleotide Phosphate Oxidase-Dependent Reactive Oxygen Species Generation in Hemodialysis Patients

Marica Cariello,[1,*] Simona Simone,[1,*] Antonia Loverre,[1] Margherita Gigante,[1] Francesca Incampo,[2] Stefania Pietanza,[1] Mario Colucci,[2] Francesco P. Schena,[1] Loreto Gesualdo,[1] Giuseppe Grandaliano,[3] and Giovanni Pertosa[1]

Abstract

Aims: This study investigated on (i) the role of gp91^{phox}/NOX2 in reactive oxygen species (ROS) generation in hemodialysis (HD) patients, and (ii) the link between clotting activation and ROS production in this setting. ***Results:*** The study was performed on peripheral blood mononuclear cells (PBMCs) isolated from HD patients randomized to polysulphon/polyamide (S-group, $n = 30$) or ethylene-vinyl-alcohol (EVAL) membrane (E-group, $n = 30$) treatment and from healthy subjects (control group, $n = 15$). ROS generation was increased in PBMCs of HD patients compared with healthy subjects. S-group showed higher levels of intracellular ROS generation than control, whereas E-group did not. In addition, S-group displayed an increase in nicotinamide adenine dinucleotide phosphate (NADPH) oxidase activity compared with E-group and healthy subjects. A further increase in NADPH activity shortly after HD treatment was observed only in S-group. The plasma levels of the prothrombin fragment F1+2, a marker of *in vivo* clotting activation, were significantly higher in S-group than in E-group. Moreover, a heightened thrombin generation was recorded in the plasma of S-group. Intracellular ROS production correlated with NADPH oxidase activity and coagulation priming in HD patients. The *in vitro* validation study demonstrated that incubation of PBMCs with activated FX induced a significant increase in intracellular ROS production, superoxide generation, and gp91^{phox}/NOX2 expression. ***Innovation:*** The pivotal role of NADPH oxidase in the upregulation of ROS in HD patients makes this enzyme a potential target for therapeutic intervention in the treatment of HD-related oxidative stress. ***Conclusion:*** The EVAL membrane, by reducing clotting activation, inhibits gp91^{phox}/NOX2-related ROS production in HD patients. *Antioxid. Redox Signal*. 16, 428–439.

Introduction

Oxidative stress plays a critical role in the pathogenesis of vascular disease (5). In hemodialysis (HD) patients, reactive oxygen species (ROS) are overproduced and antioxidant defense mechanisms are impaired (5).

The nicotinamide adenine dinucleotide phosphate (NADPH) oxidase complex is the major source of superoxide production in phagocytes and vascular tissue (28). An upregulation of the NADPH oxidase activity leads to oxidative stress (2, 34).

The NADPH oxidase complex is an enzyme that consists of several subunits: gp91^{phox}/NOX2 and p22^{phox}, the membrane bound subunits; p47^{phox}, the "organizer subunit"; p67^{phox}, the "activator subunit"; p40^{phox} and GTPase Rac, the cytosolic factors of the complex. Upon activation, there is an exchange of GDP for GTP on Rac leading to its activation. Phosphorylation of p47^{phox} induces conformational changes allowing interaction with p22^{phox}. The movement of p47^{phox} brings with it p67^{phox} and p40^{phox}, to form the active enzyme complex able to produce superoxide (3, 15, 33).

Activation of the clotting system commonly occurs during HD leading to the generation of thrombin and activated factor X (FXa) (29). Subclinical clotting activation contributes to HD-related chronic microinflammation, and thus the use of a less thrombogenic membrane, such as ethylene-vinyl-alcohol (EVAL), may improve this condition (27). EVAL is a synthetic polymer having both hydrophilic and hydrophobic segments. The hydrophilic segments are considered to reduce

[1]Renal, Dialysis and Transplantation Unit, Department of Emergency and Organ Transplantation, University of Bari, Bari, Italy.
[2]Section of General and Experimental Pathology, Department of Biomedical Sciences and Human Oncology, University of Bari, Bari, Italy.
[3]Department of Biomedical Sciences, University of Foggia, Foggia, Italy.
*These authors equally contributed to this work.

Innovation

Oxidative stress plays a critical role in the pathogenesis of atherosclerosis. Poor biocompatibility of dialytic systems has been suggested to play a key role in the enhancement of reactive oxygen species (ROS) production during hemodialysis (HD). In the current study we demonstrate, for the first time, that gp91^{phox}/NOX2-based nicotinamide adenine dinucleotide phosphate (NADPH) oxidase is involved in HD-induced ROS production by peripheral blood mononuclear cells (PBMCs), and provide evidence suggesting an association between clotting activation, in particular, FXa generation, and oxidative stress. Moreover, we show that the use of ethylene-vinyl-alcohol, a synthetic membrane displaying lesser clotting activity than polysulphon/polyamide membranes, is associated with little oxidative stress and clotting activation. Finally, the central role of NADPH oxidase in the upregulation of ROS in HD patients suggests that this enzyme may represent a molecular target for therapeutic intervention in the treatment of HD-related oxidative stress. Long-term prospective studies are warranted to confirm the link between the molecular mechanism identified in our study and the HD-related cardiovascular complications.

blood–membrane interaction and prevent adsorption of proteins, platelets, medication, and anticoagulant (4). Dialysis with EVAL is associated with a lower degree of platelet reactivity and neutrophil/monocyte activation (31). Thrombin induces oxidative stress in hippocampal neurons *in vivo* through the upregulation of gp91^{phox}/NOX2, p47^{phox}, and p67^{phox} and the consequent activation of microglial NADPH oxidase complex (6). It has recently been demonstrated that in human endothelial cells thrombin stimulates ROS generation by activating NADPH oxidase (15).

The aim of our study was to investigate the involvement of the NADPH oxidase in overproduction of ROS in patients treated with HD membranes with different biocompatibility and to evaluate the possible link between coagulation priming and ROS production.

Results

Polysulphon/polyamide membrane increases ROS production in HD patients

We measured ROS production in peripheral blood mononuclear cells (PBMCs) freshly isolated from HD patients and healthy subjects. ROS generation was significantly greater in HD patients than in controls (Fig. 1A). However, when HD patients treated with polysulphon/polyamide (S-group) or EVAL membranes (E-group) were analyzed separately, only the S-group showed a significantly higher ROS production compared with controls (Fig. 1C). Preincubation with the ROS scavenger, N-acetylcysteine (NAC), and NADPH oxidase inhibitor diphenyleneiodonium chloride (DPI) significantly inhibited ROS production (Fig. 1B–D). To investigate the involvement of the mitochondrial respiratory complexes in ROS generation, we incubated PBMCs isolated from HD patients and controls with a specific mitochondrial inhibitor Rotenone. Rotenone did not reduce ROS production in both E- and S-groups (Fig. 1E).

NADPH oxidase activity is increased in patients treated with synthetic membrane

To investigate the role of NADPH oxidase in ROS generation, we tested its activity in PBMCs of HD patients. NADPH-dependent superoxide generation was significantly increased in PBMCs of HD patients compared with controls (Fig. 2A). Interestingly, S-group showed an increase in NADPH oxidase activity compared with both E-group and control group (Fig. 2B). No difference between E-group and control group was observed (Fig. 2B). Incubation with DPI and superoxide dismutase (SOD) significantly decreased NADPH oxidase activity in the E-group (Fig. 2C). Treatment with Rotenone produced a slight, but not significant, reduction in NADPH-dependent superoxide generation in the E-group, suggesting a role for NADPH oxidase in ROS production in these patients (Fig. 2C). Next, we analyzed NADPH-dependent superoxide generation at the beginning (t0) and at the end (t240 min) of HD treatment. A significant increase of the NADPH oxidase activity after HD treatment was observed only in the S-group (Fig. 2D). We evaluated the change in NADPH/NADP$^+$ ratio in HD patients and controls and we observed a significant decrease in both E- and S-groups compared with control group, confirming that in these patients there is a continuous waste of NADPH due to chronic stimulation by HD (control group: 9.19 ± 2.54; E-group: 2.75 ± 1.76; S-group: 1.87 ± 0.8; $p = 0.002$ *vs.* E-group; $p = 0.001$ *vs.* S-group).

NADPH oxidase complex protein expression is upregulated in PBMCs of HD patients

The expression of the NADPH oxidase subunits, gp91^{phox}/NOX2 and p22^{phox}, was investigated by Western blot analysis in PBMCs isolated from HD patients and healthy subjects. HD treatment significantly increased both gp91^{phox}/NOX2 and p22^{phox} protein expression (Fig. 3A, C). An upregulation of these subunits was observed both in S- and E-groups (Fig. 3B, D) confirming a continuous production of NADPH oxidase subunits.

The use of polysulphon/polyamide membranes induces NADPH oxidase complex activation

To verify the activation of NADPH oxidase complex we immunoprecipitated Rac, a small GTPase that leads to the activation of the complex, followed by immunoblotting to gp91^{phox}/NOX2. We observed a significant increase of gp91^{phox}/NOX2 association with Rac in the S-group compared with E and control groups (Fig. 3E). The activation of the NADPH oxidase complex requires translocation of cytosolic factors to the membrane surface. To confirm this process, we analyzed the localization of NADPH oxidase subunits, gp91^{phox}/NOX2, p67^{phox}, and Rac, in PBMCs isolated from HD patients and controls by triple immunofluorescence. The colocalization of the three subunits on the membrane surface was observed only in PBMCs isolated from S-group (Fig. 4A–C). These findings further confirm that NADPH oxidase complex is activated only in patients treated with S membranes.

Clotting activation is increased in patients treated with polysulphon/polyamide membrane

We evaluated the *in vivo* activation of coagulation measuring the plasma levels of prothrombin F1 + 2, a fragment

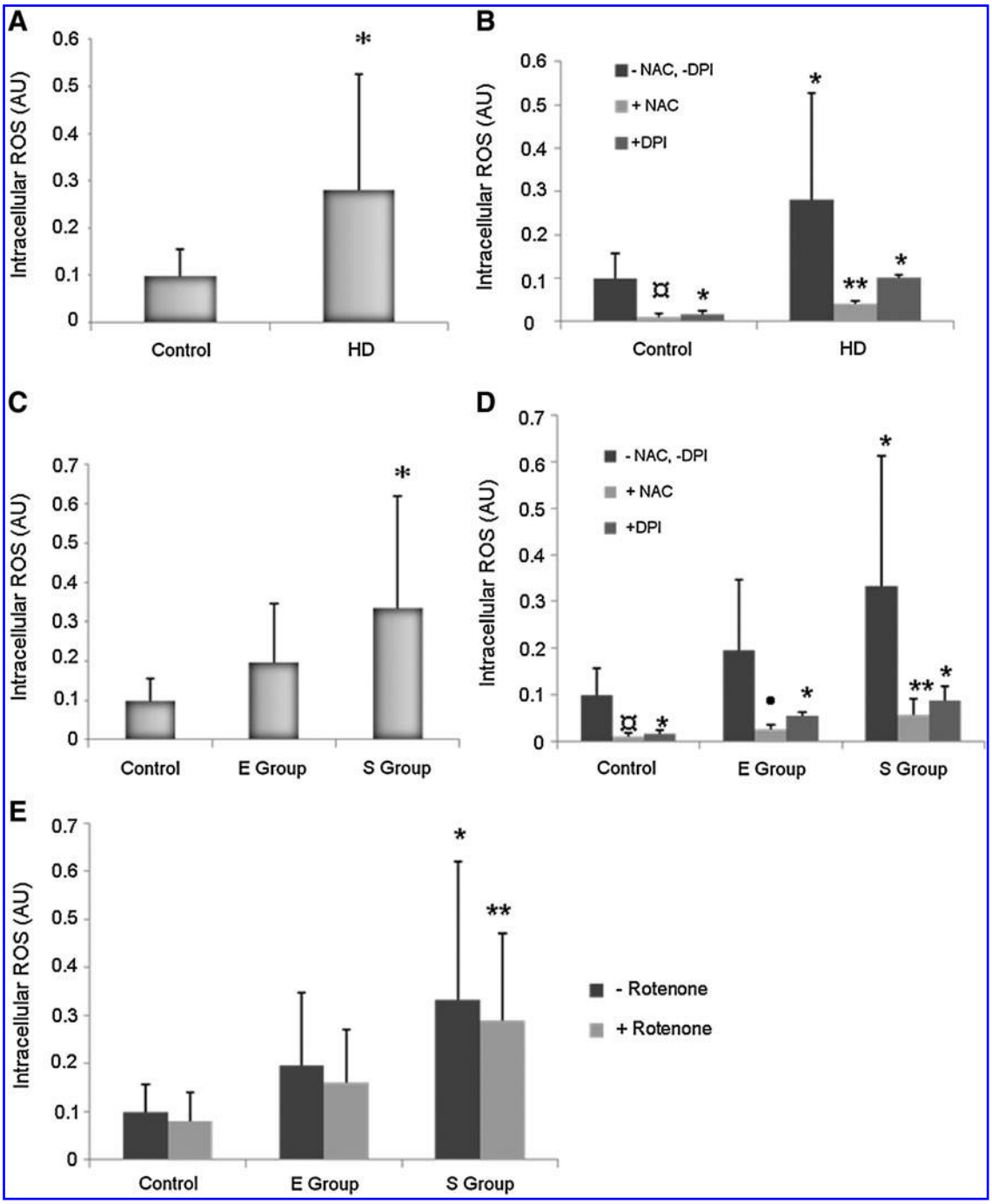

FIG. 1. ROS production in HD patients and healthy subjects. Intracellular ROS levels were investigated by DCF-DA in PBMCs isolated from healthy subjects (controls, $n=15$), and HD patients treated with polysulphon/polyamide (S-group, $n=30$) and EVAL (E-group, $n=30$) as described in Material and Methods section. ROS generation was significantly increased in PBMCs from HD patients as compared with control $^{*}p=0.001$ **(A)**. S-group, but not E-group, showed significantly higher levels of intracellular ROS generation than control $^{*}p=0.03$ **(C)**. Preincubation with an ROS scavenger NAC (5 n*M*) and NADPH oxidase inhibitor DPI (10 μM) significantly inhibited ROS production in PBMCs isolated from control, HD patients, S-group, and E-group as compared with NAC, DPI condition, $p<0.01$ **(B, D)**. A slight, but not significant, reduction in ROS production was observed in PBMCs isolated from control, S-group, and E-group treated with a mitochondrial inhibitor Rotenone (10 μM). S-group treated with Rotenone showed significantly higher levels of intracellular ROS production than controls treated with Rotenone $^{**}p=0.02$ **(E)**. Results are means ± SD. DCF-DA, 2′,7′-dichlorodihydrofluorescein diacetate; DPI, diphenyleneiodonium chloride; EVAL, ethylene-vinyl-alcohol; HD, hemodialysis; NAC, N-acetylcysteine; NADPH, nicotinamide adenine dinucleotide phosphate; PBMCs, peripheral blood mononuclear cells; ROS, reactive oxygen species; SD, standard deviation.

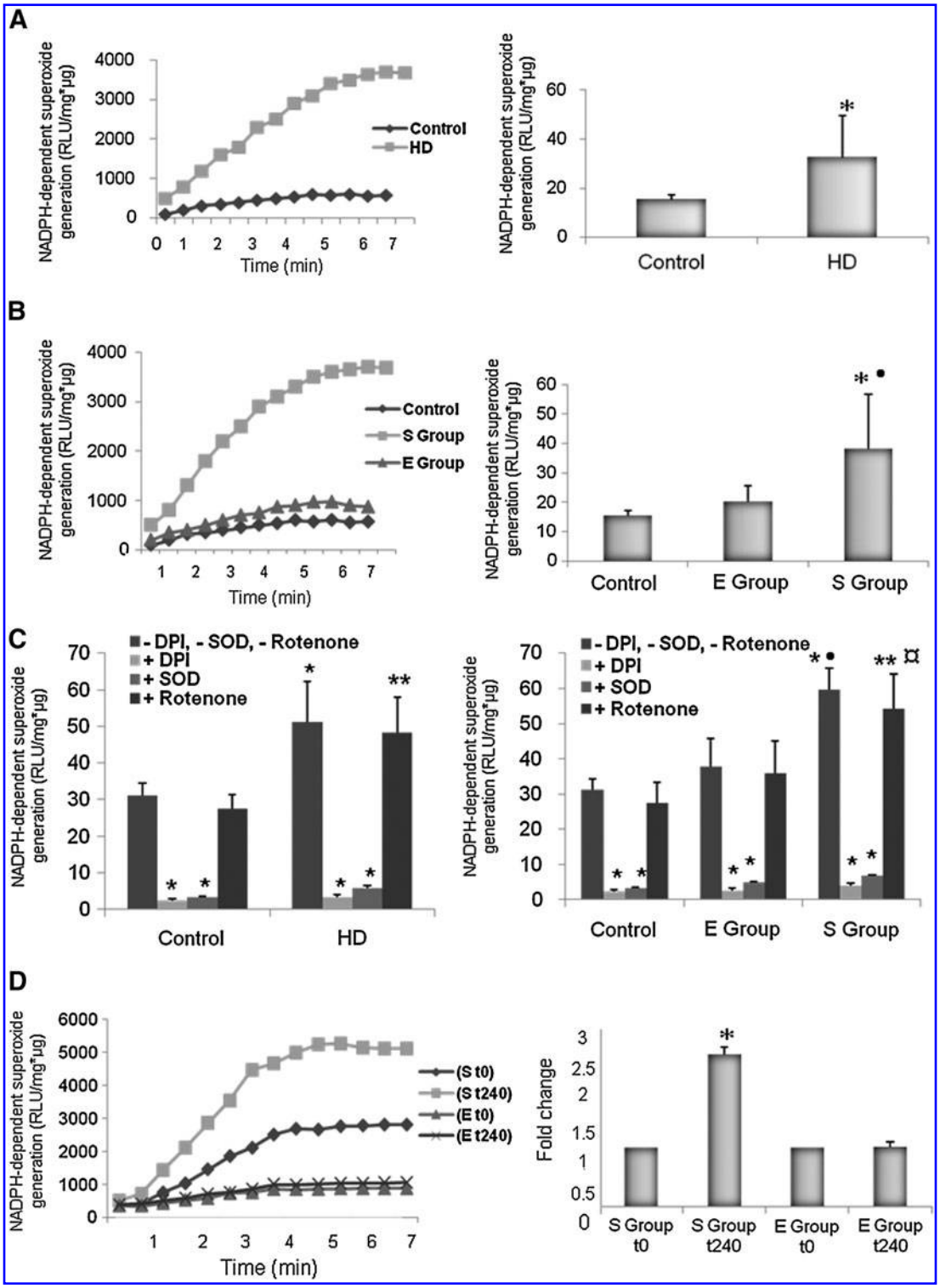

FIG. 2. NADPH-dependent superoxide generation in HD patients and controls. NADPH oxidase activity was measured by lucigenin-enhanced chemiluminescence in PBMCs isolated from HD patients and healthy subjects (controls) and HD patients subsequently treated with polysulphon/polyamide (S-group) and EVAL (E-group). NADPH oxidase activity was significantly increased in PBMCs from HD patients $^{*}p = 0.04$ *versus* control **(A)**. S-group showed an increase in NADPH-dependent superoxide generation as compared with E-group and control group ($^{*}p = 0.01$ *vs.* control; $\bullet p = 0.05$ *vs.* E-group; **B)**. Preincubation with NADPH oxidase inhibitor DPI (10 μM) and SOD (50 μg/ml) significantly decreased NADPH oxidase activity in PBMCs isolated from control, HD patients, S-group, and E-group $^{*}p < 0.01$ **(C)**. Pretreatment with Rotenone (10 μM) produced a slight, but not significant, reduction in NADPH-dependent superoxide generation in PBMCs from control, HD patients, S-group, and E-group. HD patients and S-group treated with Rotenone showed an increase in NADPH-dependent superoxide generation compared with E-group and control group treated with Rotenone ($^{**}p = 0.03$ *vs.* control; $^{\circ}p = 0.04$ *vs.* E-group; **C)**. Results are shown as means ± SD. NADPH-dependent superoxide generation was analyzed at the beginning and at the end of HD treatment. An increase of enzyme activity after HD treatment was observed only in the S-group ($^{*}p = 0.04$). Results are shown as fold change ± SEM **(D)**; control group $n = 15$; E-group $n = 30$, S-group $n = 30$. SEM, standard error of the mean; SOD, superoxide dismutase.

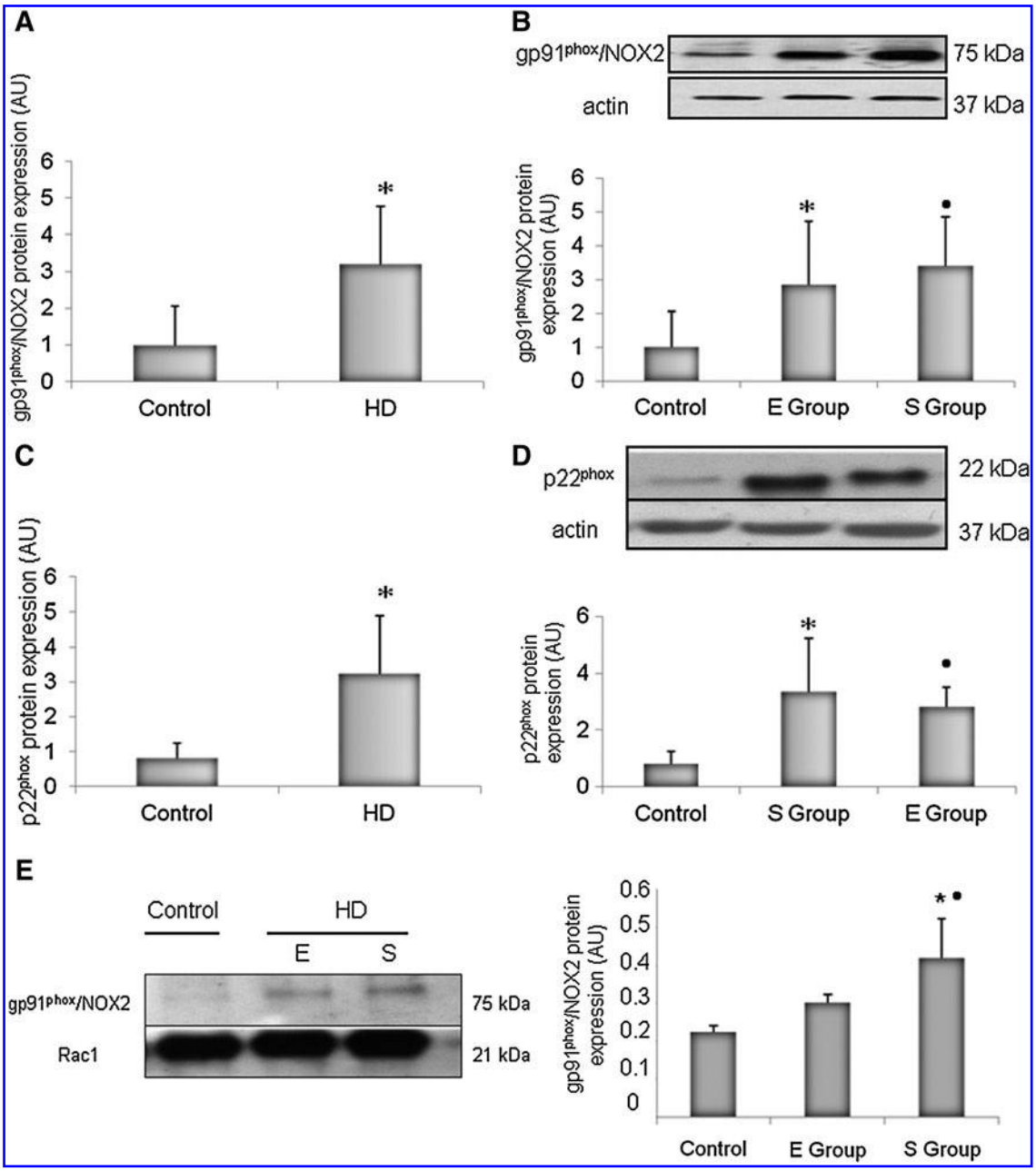

FIG. 3. NADPH oxidase complex protein expression. Gp91^{phox}/NOX2 and p22^{phox} protein expression was analyzed by immunoblotting in PBMCs isolated from HD patients treated with polysulphon/polyamide (S-group), EVAL (E-group), and controls. Quantification of gp91^{phox}/NOX2 immunoblotting: *$p = 0.0009$ *versus* control **(A)**; *$p = 0.02$ *versus* control, •$p = 0.005$ *versus* control **(B)**. Quantification of p22^{phox} immunoblotting: *$p = 0.0002$ *versus* control **(C)**; *$p = 0.0008$ *versus* control, •$p = 0.00004$ *versus* control **(D)**. Immunoprecipitation for Rac followed by immunoblotting to gp91^{phox}/NOX2 showed the activation of NADPH oxidase complex. We observed an increase of gp91^{phox}/NOX2 in S-group as compared with controls and E-group. Quantification of gp91^{phox}/NOX2 immunoblotting/Rac1 immunoprecipitation: *$p = 0.01$ *versus* control and •$p = 0.04$ *versus* E-group **(E)**. Results are means ± SD; control group $n = 15$; E-group $n = 30$, S-group $n = 30$.

released from prothrombin during FXa-catalyzed conversion to thrombin. F1 + 2 levels were significantly higher in S-group than in E-group (Fig. 5A). Moreover, we assayed the endogenous thrombin potential using a functional assay that measures the kinetics of thrombin generation and disappearance in plasma upon activation of coagulation by a low concentration of tissue factor (16). The peak of thrombin generation was significantly higher in S-group, suggesting a greater thrombin-forming capacity (Fig. 5B).

Intracellular ROS production correlates with NADPH oxidase activity and coagulation activation in HD patients

NADPH oxidase activity and plasma levels of prothrombin F1 + 2 directly and significantly correlated with intracellular ROS production in HD patients ($r = 0.57$, $p = 0.04$; and $r = 0.85$, $p = 0.03$, respectively). Moreover, NADPH oxidase activity directly correlated with coagulation priming in HD patients ($r = 0.89$, $p = 0.0006$).

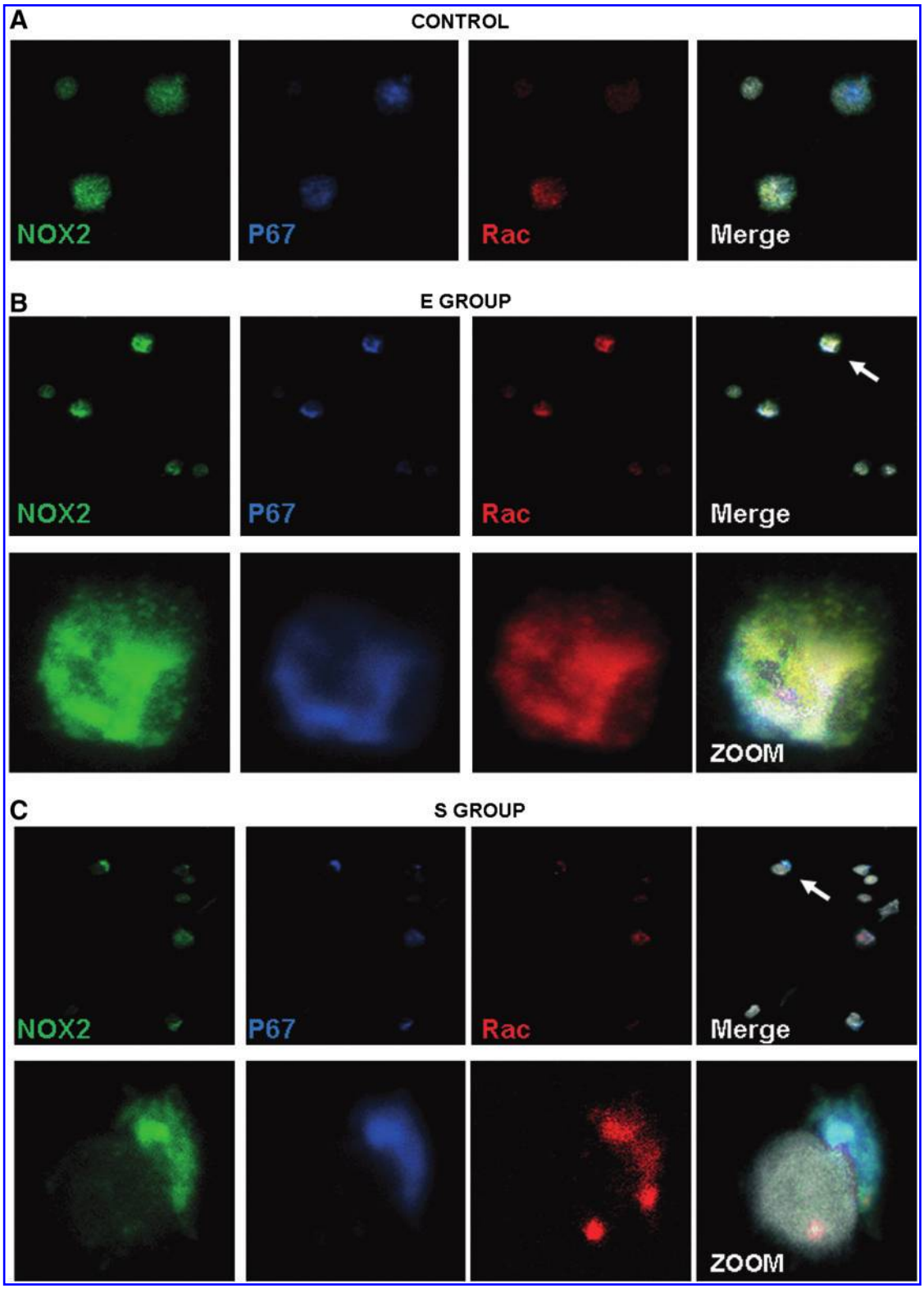

FIG. 4. Coexpression of gp91^{phox}/NOX2, p67^{phox}, and Rac in HD patients and healthy subjects. Representative image of PBMCs isolated from HD patients treated with EVAL (E-group) **(B)**, polysulphon/polyamide (S-group) **(C)**, and control **(A)** showing a colocalization of NADPH oxidase subunits, gp91^{phox}/NOX2 (green), p67^{phox} (blue), and Rac (red), by triple immunofluorescence. Nuclei were stained with Sytox (cyan). The arrows indicate the enlarged cells in the zoom. Magnification $\times 63$. Control group $n=5$; E-group $n=5$, S-group $n=5$.

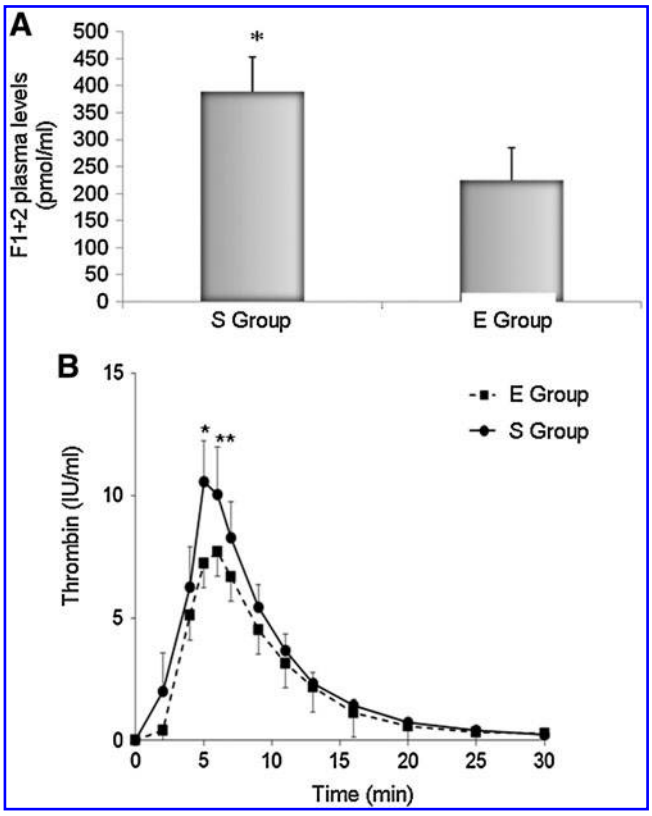

FIG. 5. Coagulation activation in HD patients. Plasma levels of prothrombin fragment F1 + 2 were higher in S-group than in E-group ($p < 0.01$, $n = 30$ per group), suggesting a greater *in vivo* clotting activation **(A)**. *In vitro* thrombin generation curves in plasma challenged with a low concentration of tissue factor. Peak thrombin activity was significantly higher in S-group as compared with E-group (*$p = 0.02$, **$p = 0.02$, $n = 10$ per group; **B)**. Results are means ± SD.

FXa increases NADPH oxidase activity and protein expression in cultured PBMCs

To investigate whether the coagulation activation is involved in intracellular ROS production and in the NADPH oxidase complex activation, we stimulated PBMCs isolated from healthy subjects with FXa (10 n*M*) at different time periods (10, 20, 30, and 60 min). Intracellular ROS production, NADPH-dependent superoxide generation, and $gp91^{phox}$/NOX2 protein expression peaked at 30 min and decreased after 60 min of FXa incubation (Fig. 6A, C, E). Preincubation with NAC and DPI significantly inhibited ROS production in PBMCs stimulated with FXa for 30 min (Fig. 6B). Preincubation with Rotenone did not significantly reduce ROS production and NADPH-dependent superoxide generation (Fig. 6B, D). Preincubation with DPI and SOD significantly inhibited NADPH oxidase activity in PBMCs stimulated with FXa (Fig. 6D).

Discussion

In the current study we demonstrated for the first time that $gp91^{phox}$/NOX2-based NADPH oxidase is involved in HD-induced oxidative stress and provided evidence suggesting that such event is associated to the activation of the coagulation cascade. Accordingly, the use of EVAL, a low coagulation-activating membrane, significantly reduces NADPH oxidase activity and ROS generation.

Archetypal cardiovascular risk factors have been associated with high incidence of cardiovascular disease–featuring HD patients (18). These traditional risk factors, however, appear to explain only partially the increased burden of cardiovascular disease in these population (32). Oxidative stress has been proposed as a nontraditional cardiovascular risk factor in this setting, and has been well documented in HD patients (21, 22, 26).

The generation of ROS, including nitric oxide and peroxynitrite, during HD is associated with PBMC activation (21, 22, 26). The bioincompatibility of the dialytic system has been suggested to play a key role in the enhancement of ROS production (8, 9, 12). We previously demonstrated that JNK phosphorylation, an oxidative stress-induced protein kinase, is strikingly increased in PBMCs of patients treated with cellulosic membrane. This process may represent an important mechanism in PBMC activation during HD using bioincompatible devices (26). In the current study, we observed an ROS overproduction by PBMCs isolated from HD patients. In particular, patients treated with polysulphon/polyamide membranes showed a significant increase of ROS production, although these dialyzers have been shown to reduce the priming of the complement cascade and the activation of PBMCs compared with cellulose-based membranes. Interestingly, ROS generation in patients treated with EVAL membranes did not differ from control group, suggesting that the use of EVAL could reduce the oxidative stress in HD patients through mechanisms other than direct or complement-mediated PBMC activation.

NADPH oxidase is an example of enzyme potentially responsible for ROS overproduction. Mitochondria stand at the center of cellular ROS metabolism being, at the same time, the major producer and the primary target of prooxidant molecules. The activated NADPH oxidase complex catalyzes the reduction of molecular oxygen to superoxide anion, which, in turn, dismutates to form hydrogen peroxide, a reaction catalyzed by SOD. Measurement of NADPH oxidase activity is traditionally performed on the plasma membrane fraction. Although we feel that this approach would have been useful to confirm our working hypothesis, to measure NADPH oxidase activity directly on plasma membranes requires approximately $3–4 \times 10^8$ cells, corresponding to 200 ml of whole blood (1). Harvesting this blood volume from anemic HD patients (mean Hb of our patient population is 10.2 g/dl) is ethically challenging. In the attempt to overcome this limit NADPH oxidase activity was measured in whole cell fractions in the presence and in the absence of enzyme and mitochondrial inhibitors (DPI and Rotenone, respectively). We observed a significant upregulation of NADPH-dependent superoxide generation in PBMCs isolated from patients treated with polysulphon/polyamide membranes compared with EVAL-treated patients and healthy subjects. Interestingly, a further increase in NADPH oxidase activity was observed at the end of HD treatment only in patients treated with polysulphon/polyamide membranes, confirming the hypothesis that the activation of this prooxidative pathway is directly linked to the use of a specific membrane. To confirm the activation of NADPH oxidase complex we analyzed

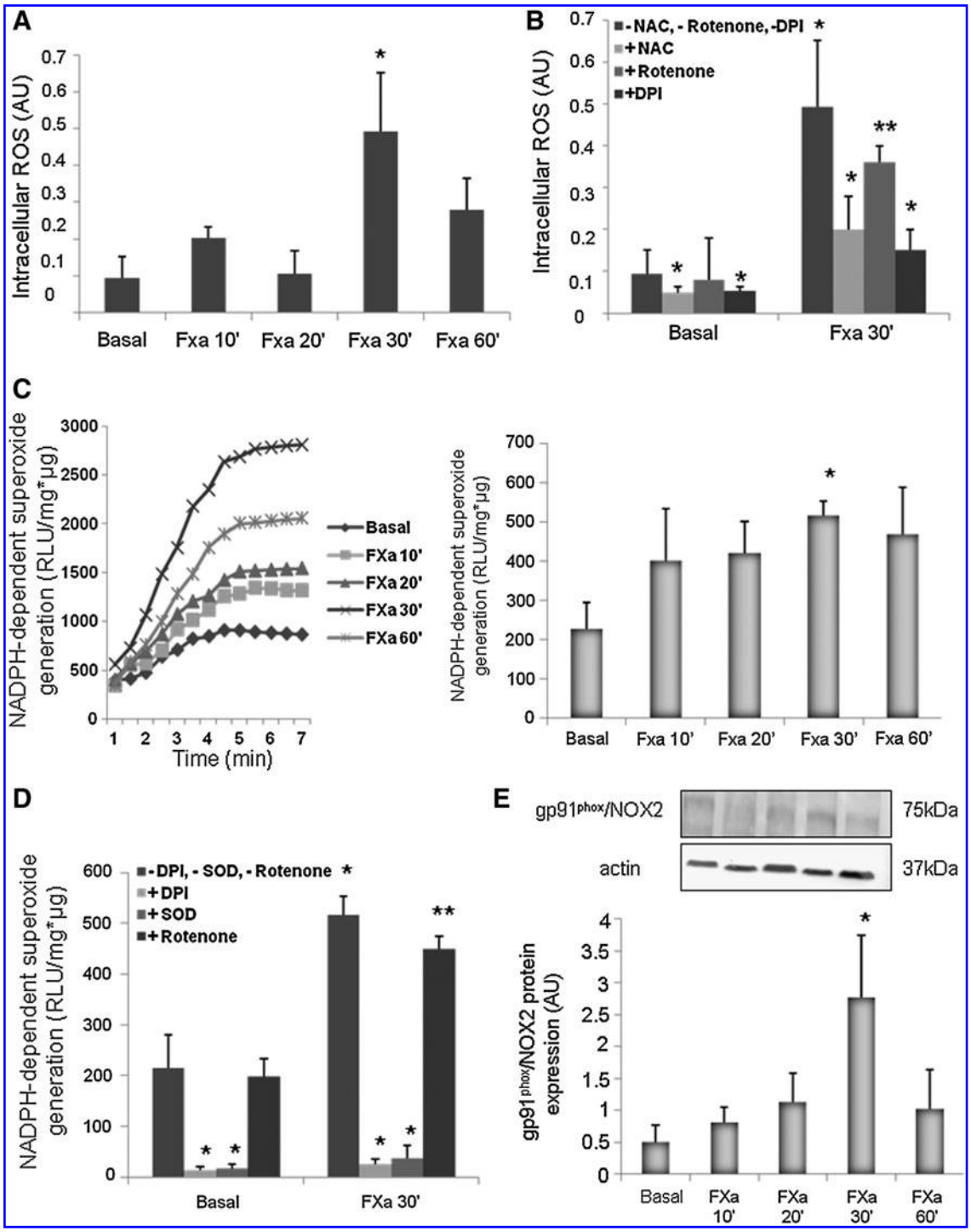

FIG. 6. Coagulation activation induced NADPH oxidase complex. PBMCs isolated from buffy coat were incubated with FXa (10 n*M*) for 10–60 min. Intracellular ROS levels were investigated by DCF-DA. *$p = 0.01$ *versus* basal; $n = 4$ **(A)**. Preincubation with NAC and DPI significantly inhibited ROS production in PBMCs stimulated with FXa for 30 min as compared with NAC, Rotenone, and DPI condition, *$p < 0.01$, $n = 3$ **(B)**. Preincubation with Rotenone (10 μM) did not significantly decreased ROS production and these cells showed a significant upregulation compared with basal pretreated with Rotenone, **$p = 0.03$, $n = 4$ **(B)**. NADPH oxidase activity was measured by lucigenin-enhanced chemiluminescence. *$p = 0.01$ *versus* basal; $n = 3$ **(C)**. Preincubation with DPI (10 μM) and SOD (50 μg/ml) significantly inhibited NADPH oxidase activity in PBMCs stimulated with FXa for 30 min, *$p < 0.01$, $n = 3$ **(D)**. Preincubation with Rotenone did not significantly decrease NADPH oxidase activity and these cells showed a significant upregulation compared with basal pretreated with Rotenone, **$p = 0.02$, $n = 3$ **(D)**. Gp91^{phox}/NOX2 protein expression was studied by immunoblotting for gp91^{phox}/NOX2. *$p = 0.03$ *versus* basal; $n = 3$ **(E)**. Results are means ± SD.

gp91^{phox}/NOX2 and p22^{phox} protein expression and immunoprecipitated Rac, a small GTPase that leads to the activation of the enzymatic complex, followed by immunoblotting with specific anti-gp91^{phox}/NOX2 antibodies. A similar pattern of protein expression was observed both in E- and S-groups. This observation might be explained by the chronic microinflammation featuring HD, which has been shown to be associated with a positive feedback of continuous p22^{phox} synthesis (11). However, the colocalization of NADPH subunits, gp91^{phox}/NOX2, p67^{phox}, and Rac, on the membrane surface of PBMCs isolated only from S-group, further confirmed that NADPH oxidase complex is activated in patients treated with these synthetic dialytic membranes, but not in those treated with EVAL. Next, we observed a nonsignificant reduction of NADPH/NADP$^+$ ratio in S-group as compared with E-group, supporting the hypothesis that there is a continuous waste of NADPH in HD patients.

HD-related oxidative stress relies on two major components of the dialysis system: the dialyzer (35), and the microbial contamination and/or the pyrogen content of the dialysate. In particular, the presence of LPS in the dialysate may activate monocytes/macrophages (19, 20) and NADPH oxidase complex upregulation (21, 25, 30). Recently, Morena *et al.* showed that the lowering dose of systemic LMW heparin in patients dialyzed with a new heparin-coated Evodial was associated with a prevention of oxidative status. Moreover, the authors stated that heparin may act as a prooxidant agent increasing oxidative stress, but the use of unfractionated heparin has not been tested in this work (23). In a previous study, we demonstrated that subclinical clotting activation caused an increased CCR2 gene expression in uremic PBMCs; the use of EVAL improved this condition by reducing specific FXa and MCP-1 cell surface receptors (27). In this study we showed that patients treated with EVAL had significantly lower plasma levels of prothrombin F1+2, suggesting a low blood clotting activation. Moreover, we demonstrated that the *in vitro* thrombin-forming capacity was lower in the E-group than in the S-group, suggesting a more pronounced hypercoagulable state in the latter. Thus, it is conceivable that the increased NADPH activity observed in the S-group might be linked to the heightened activation of the coagulation cascade. This hypothesis is supported by the direct and significant correlation between intracellular ROS production, NADPH oxidase activity, and coagulation activation.

NADPH oxidase activation may play a crucial role in perpetuating the thrombogenic cycle in the injured vessel wall (17). Thrombin-induced ROS production and vascular smooth muscle cell proliferation were significantly reduced after downregulation of NoxA1, a functional homolog of p67^{phox} (24). In addition, thrombin stimulates NOX-dependent ROS generation in endothelial cells, through Rac1 activation and gp91^{phox}/NOX2 upregulation, promoting endothelial proliferation and angiogenic response (10). It has been demonstrated that thrombin induces the upregulation of gp91^{phox}, p47^{phox}, and p67^{phox} proteins and causes the translocation of cytosolic NADPH oxidase subunits (p47^{phox}, p67^{phox}, and Rac1) to the plasma membrane in microglia within the hippocampus *in vivo* (6). Our *in vitro* experiments would suggest that thrombin is not the only coagulation factor promoting ROS generation. Indeed, in our *in vitro* experiments we observed that FXa was able to induce intracellular ROS production, NADPH-dependent superoxide generation, and gp91^{phox}/NOX2 protein expression in PBMCs isolated from healthy subjects.

In conclusion, our data support the hypothesis that subclinical clotting activation may cause an increase of NADPH-related ROS production in PBMCs of HD patients. The use of EVAL membrane improves this condition likely by reducing the generation of FXa. The pivotal role of NADPH oxidase in the upregulation of ROS makes this enzyme a potential target for therapeutic intervention in the treatment of HD-related oxidative stress occurring in uremic patients.

Materials and Methods

Patients

Thirty HD patients, after giving a written informed consent according to the declaration of Helsinki, were enrolled based on the following inclusion/exclusion criteria: >18 years, stably on HD for at least 1 year, no signs of liver disease, dysregulations of coagulation system, diabetes, systemic inflammatory disease, vasculitides, or neoplasia. Underlying diseases leading to end-stage renal disease were chronic glomerulonephritis in 8 patients (26.6%), hypertensive nephrosclerosis in 12 (40%), polycystic kidney disease in 4 (13.3%), tubulointerstitial nephritis in 5 (16.6%), and unknown disease in 1 (3.3%). HD patients (12 women and 18 men; mean age 46.5±10.8 years) were dialyzed for at least 6 months with synthetic membranes (polysulphon, Fresenius, Bad Homburg, Germany; or polyamide, Gambro, Bologna, Italy; S-group, $n=30$). The patients were switched from polysulphon/polyamide to EVAL (Kuraray, Tokyo, Japan; E-group, $n=30$) for 36 treatments and vice versa for another 36 treatments. Fifteen healthy subjects (eight women and seven men; mean age 43.2±11.2 years) were used as control group. HD patients and controls were matched for gender and age. No medications (antiinflammatory and antihypertensive drugs, corticosteroids, and vitamin C-E) potentially interfering with the parameters under investigation were administered throughout the study. All patients received 1250 U/h of sodium heparin infusion during HD. No difference in the dose of erythropoiesis-stimulating agents was present between E and S-groups. No significant difference in the proportions of lymphocytes/monocytes in each sample was observed. HD efficiency, as indicated by urea reduction rate, remained unchanged during the study periods. Dialyzers were not reused. Endotoxin content of the dialysate, as shown by colorimetric Limulus Amebocyte Lysate assay (Coatest Kabi Vitrum, Stockholm, Sweden), was constantly <0.05 EU/ml.

Antibodies

The primary antibodies used in this study recognize NADPH oxidase complex subunits: rabbit polyclonal anti-human gp91^{phox}/NOX2 (1:200) used for Western blot and immunoprecipitation analysis (Millipore, Bedford, MA), mouse monoclonal anti-human gp91^{phox}/NOX2 used for immunofluorescence, mouse monoclonal anti-human p67^{phox} (BD Biosciences, Franklin Lakes, NJ), rabbit polyclonal anti-human p22^{phox} (1:200; Santa Cruz Biotechnology, Santa Cruz, CA), mouse monoclonal anti-human Rac1 clone23A8 (1:1000) used for immunoprecipitation, rabbit polyclonal anti-human Rac1b used for immunofluorescence (Millipore); mouse monoclonal anti-human β-actin, used for Western blotting

(clone AC-15, 1:10,000; Sigma-Aldrich, St. Louis, MO). Secondary antibodies used in this study were as follows: horseradish peroxidase-conjugated antibodies (goat anti-rabbit IgG sc-2004 for gp91^{phox}/NOX2 and p22^{phox}, respectively, 1:1000 or 1:5000, from Santa Cruz Biotechnology; goat anti-mouse IgG for β-actin and Rac1 clone 23A8 1:50,000, from Bio-Rad Laboratories, Hercules, CA).

PBMC isolation

Whole blood was collected from all subjects. For HD patients the blood samples were obtained at the beginning (t0) and at the end (t240) of the second HD session of the week. PBMCs were isolated by density separation over a Ficoll-Paque (GE Healthcare, Stockholm, Sweden). Cells were counted and their viability was assessed by trypan blue exclusion (>90% PBMCs were viable). For the *in vitro* study, PBMCs were isolated from buffy coat obtained from healthy subjects.

In vitro *experiments*

PBMCs isolated from healthy subjects were preincubated in serum-free RPMI-1640 (Lonza, Milan, Italy) overnight and then exposed to FXa (10 n*M*; Calbiochem, La Jolla, CA) for the indicated time periods. In separate experiments PBMCs were preincubated with NAC (5 n*M*; Sigma, Milan, Italy), Rotenone (10 μM; Sigma), or DPI (10 μM) for 1 h.

Measurement of intracellular ROS production

The oxidation-sensitive fluorescent probe 2′,7′-dichlorodihydrofluorescein diacetate (DCF-DA; Molecular Probes, Eugene, OH) was used to detect the generation of intracellular ROS as described previously (13). PBMCs were maintained in culture medium (RPMI-1640; Sigma) supplemented with 10% fetal bovine serum (Sigma), 1% penicillin–streptomycin, and 2 m*M* L-glutamine for 2 h. The cells were, then, washed with Hanks' balanced salt solution (HBSS) without phenol red and incubated with 10 μM DCF-DA for 30 min in the dark at 37°C. DCF fluorescence was detected at excitation of 495 nm and emission of 525 nm wavelengths, with a fluorescence reader (JASCO-FP-6200, Tokyo, Japan). Emitted fluorescence was normalized to the total amount of proteins.

NADPH oxidase assay

NADPH oxidase activity was measured by the lucigenin-enhanced chemiluminescence method as reported previously (14). PBMCs were washed in PBS and harvested in lysis buffer (20 m*M* KH_2PO_4, pH 7.0; 1 m*M* EGTA; 1 m*M* PMSF; and 8 μg/ml leupeptin) on ice. Homogenates were subjected to a low-speed centrifugation (800 *g*) at 4°C for 10 min to remove cell debris, and used immediately. One hundred microliters of homogenates was added to 900 μl of 50 m*M* phosphate buffer, pH 7.0, containing 1 m*M* EGTA, 150 m*M* sucrose, 5 μM lucigenin, and 100 μM NADPH (Roche Diagnostic, Mannheim, Germany), when required SOD (50 μg/ml) was added to the assay. Photon emission in terms of relative light units was measured every 30 s for 7 min in a luminometer. A buffer blank was subtracted from each reading. Superoxide production was expressed as the rate of relative chemiluminescence (light) units per min per μg of protein (RLU/min*μg). Protein content was measured using the Bradford method (Bio-Rad Laboratories).

NADPH/NADP$^+$ assay

NADPH/NADP$^+$ ratio was evaluated in PBMCs freshly isolated from HD patients and controls by a commercially available kit (Abcam, Cambridge, UK).

Western blot and immunoprecipitation

Cells were lysed with RIPA buffer. The lysates were kept on ice for 30 min and centrifuged at 10,000 *g* at 4°C for 10 min. Protein concentration was determined by the Bradford method (Bio-Rad Laboratories). Aliquots containing 80 μg of proteins from each sample were subjected to SDS–PAGE on a 10% gel under reducing conditions, electrotransferred onto polyvinylidene fluoride (PVDF) membrane (Millipore), and immunoblotted with the antibodies indicated previously. The signal was detected using the ECL-enhanced chemiluminescence system (Amersham, Piscataway, NJ). The film was acquired using a scanner EPSON Perfection 2580 Photo and quantified by NIH ImageJ software (http://rsbweb.nih.gov/ij/). All samples (control, S-group, and E-group) were run in a single gel and β-actin band intensity was used for equal loading control and for normalization. A total of 200 μg of protein was immunoprecipitated using the protein G immunoprecipitation kit (Sigma). The proteins were first incubated with 1 μg of anti-Rac1 clone 23A8, overnight on a rocking platform at 4°C, and then with protein G Sepharose for 3 h at 4°C. The immunoprecipitated proteins were eluted in sample buffer (2-β-mercaptoethanol, 10% SDS, 10% glycerol, 0.5 *M* Tris-HCl [pH 6.8], and 0.05% blue-bromophenol), boiled, separated by electrophoresis on a 10% polyacrylamide gel, transferred onto a PVDF membrane, and immunoblotted with the antibodies indicated as described previously. The ECL system was used for detection. All samples (control, S-group, and E-group) were run in a single gel and Rac1 clone 23A8 band intensity was used for normalization.

Assay of prothrombin F1+2 fragment

In vivo blood clotting activation was evaluated by assaying the plasma levels of the prothrombin fragment F1+2 by a commercially available ELISA (Dade Behring, Marburg, Germany), according to the manufacturer's instructions.

Thrombin generation assay

The profile of thrombin generation induced by physiological concentrations of tissue factor was determined as previously reported (7). Briefly, a mixture consisting of 0.5 ml defibrinated plasma, 5 pM Tissue factor (Recombiplastin; Instrumentation Laboratory, Milan, Italy), and 10 m*M* $CaCl_2$ was incubated at 37°C. At predetermined intervals, a 50 μl aliquot was taken and transferred to a prewarmed tube containing 100 μl human fibrinogen (6 mg/ml) dissolved in citrate-Tris buffer (0.38% sodium citrate). The clotting time was determined by the manual (tilt tube) technique, and thrombin activity was calculated by reference to a calibration curve constructed with purified human thrombin (Sigma).

Cell immunofluorescence and confocal laser-scanning microscopy

The colocalization of gp91^{phox}/NOX2, p67^{phox}, and Rac was evaluated by indirect immunofluorescence and confocal

microscopy, on PBMCs fixed in 3.7% paraformaldehyde. Cells were permeabilized in PBS with 0.25% Triton X-100 for 5 min, washed in PBS, and then blocked with 2% bovine serum albumin (BSA) in PBS for 1 h at RT. Cells were incubated overnight at 4°C with a primary antibody against gp91^{phox}/NOX2 (1:20), p67^{phox} (1:50), and Rac1b (1:400), following incubation for 1 h with the appropriate secondary antibody (Alexa Fluor 488 goat anti-mouse IgG1, 1:200; Alexa Fluor 633 goat anti-mouse, 1:400; and Alexa Fluor 555 goat anti-rabbit, 1:200, respectively; Molecular Probes) at RT. PBMCs were washed in PBS after each step, counterstained with Sytox® (Molecular Probes), mounted in GEL/MOUNT (Biomeda Corp., Foster City, CA), and sealed with nail varnish. Negative controls were performed by omitting the primary antibodies. Specific fluorescence was acquired by a Leica TCS SP2 (Leica, Wetzlar, Germany) confocal laser-scanning microscope.

Statistical analysis

Data are expressed as the mean ± standard deviation or mean ± standard error of the mean. Differences between control, HD (S + E-groups), E-, and S-groups were analyzed by ANOVA. Pearson's correlation test was used to study continuous variables. A p-value < 0.05 was considered statistically significant. Statistical analysis was performed using the Statview Software package (5.0 version; SAS, Inc., Cary, NC).

Acknowledgments

This work was funded by "Regione Puglia" (Progetto Strategico 2006 PS094/06 granted to G. Pertosa) and by the Ministero della Salute (Ricerca finalizzata granted to G. Pertosa, Progetto FIRB 2011 cod. RBAP11B2SX granted to L. Gesualdo) and by an unrestricted research grant from Roche. We thank Prof. G. Villani (Dept. of Biochemistry, University of Bari) for the valuable help in intracellular ROS measurements, Dr. M. Di Pilato (Dept. of Nephrology, University of Bari) for the excellent technical assistance, and Dr. M.P. Scavo (Dept. of Gastroenterology, University of Bari) for technical support in Confocal Laser-Scanning Microscopy.

Author Disclosure Statement

No competing financial interests exist.

References

1. Abo A, Boyhan A, West I, Thrasher AJ, and Segal AW. Reconstitution of neutrophil NADPH oxidase activity in the cell-free system by four components: p67-phox, p47-phox, p21rac1, and cytochrome b-245. *J Biol Chem* 267: 16767–16770, 1992.
2. Babior BM, Lambeth JD, and Nauseef W. The neutrophil NADPH oxidase. *Arch Biochem Biophys* 397: 342–344, 2002.
3. Bedard K and Krause KH. The NOX family of ROS-generating NADPH oxidases: physiology and pathophysiology. *Physiol Rev* 87: 245–313, 2007.
4. Bonomini M, Pavone B, Sirolli V, Del Buono F, Di Cesare M, Del Boccio P, Amoroso L, Di Ilio C, Sacchetta P, Federici G, and Urbani A. Proteomics characterization of protein adsorption onto hemodialysis membranes. *J Proteome Res* 5: 2666–2674, 2006.
5. Castilla P, Dávalos A, Teruel JL, Cerrato F, Fernández-Lucas M, Merino JL, Sánchez-Martín CC, Ortuño J, and Lasunción MA. Comparative effects of dietary supplementation with red grape juice and vitamin E on production of superoxide by circulating neutrophil NADPH oxidase in hemodialysis patients. *Am J Clin Nutr* 87: 1053–1061, 2008.
6. Choi SH, Lee DY, Kim SU, and Jin BK. Thrombin-induced oxidative stress contributes to the death of hippocampal neurons *in vivo*: role of microglial NADPH oxidase. *J Neurosci* 25: 4082–4090, 2005.
7. Colucci M, Binetti BM, Tripodi A, Chantarangkul V, and Semeraro N. Hyperprothrombinemia associated with prothrombin G20210A mutation inhibits plasma fibrinolysis through a TAFI-mediated mechanism. *Blood* 103: 2157–2161, 2004.
8. Cristol JP, Canaud B, Rabesandratana H, Gaillard I, Serre A, and Mion C. Enhancement of reactive oxygen species production and cell surface markers expression during haemodialysis. *Nephrol Dial Transplant* 9: 389–394, 1994.
9. Descamps-Latscha B, Goldfarb B, Nguyen A, Landais P, London G, Haewfneer-Cavaillon N, Jacquot C, Herbelin A, and Kazatchkine M. Establishing the relationship between complement activation and stimulation of phagocyte oxidative metabolism in hemodialyzed patients: A randomized prospective study. *Nephron* 59: 279–285, 1991.
10. Diebold I, Djordjevic T, Petry A, Hatzelmann A, Tenor H, Hess J, and Görlach A. Phosphodiesterase 2 mediates redox-sensitive endothelial cell proliferation and angiogenesis by thrombin via Rac1 and NADPH oxidase 2. *Circ Res* 104: 1169–1177, 2009.
11. Djordjevic T, Pogrebniak A, BelAiba RS, Bonello S, Wotzlaw C, Acker H, Hess J, and Görlach A. The expression of the NADPH oxidase subunit p22phox is regulated by a redox-sensitive pathway in endothelial cells. *Free Radic Biol Med* 1;38: 616–630, 2005.
12. Floridi A, Piroddi M, Pilolli F, Matsumoto Y, Aritomi M, and Galli F. Analysis method and characterization of the antioxidant capacity of vitamin E-interactive polysulfone hemodialyzers. *Acta Biomater* 5: 2974–2982, 2009.
13. Gorin Y, Kim NH, Feliers D, Bhandari B, Choudhury GG, and Abboud HE. Angiotensin II activates Akt/protein kinase B by an arachidonic acid/redox-dependent pathway and independent of phosphoinositide 3-kinase. *FASEB J* 15: 1909–1920, 2001.
14. Gorin Y, Ricono JM, Kim NH, Bhandari B, Choudhury GG, and Abboud HE. Nox4 mediates angiotensin II-induced activation of Akt/protein kinase B in mesangial cells. *Am J Physiol Renal Physiol* 285: F219–F229, 2003.
15. Groemping Y and Rittinger K. Activation and assembly of the NADPH oxidase: a structural perspective. *Biochem J* 386: 401–416, 2005.
16. Hemker HC. Recollections on thrombin generation. *J Thromb Haemost.* 6: 219–226, 2008.
17. Herkert O, Diebold I, Brandes RP, Hess J, Busse R, and Görlach A. NADPH oxidase mediates tissue factor-dependent surface procoagulant activity by thrombin in human vascular smooth muscle cells. *Circulation* 105: 2030–2036, 2002.
18. Jungers P, Nguyen Khoa T, Joly D, Choukroun G, Witko-Sarsat V, and Massy ZA. Atherosclerotic complications in chronic renal failure: epidemiology and predictive factors. *Adv Nephrol Necker Hosp* 30: 177–199, 2000.
19. Knudsen P, Leon J, Ng A, Shaldon S, Floege J, and Koch KM. Hemodialysis-related induction of beta-2microglobulin and

interleukin-1 synthesis and release by mononuclear phagocytes. *Nephron* 53: 188–193, 1989.
20. Kumano K, Yokota S, Nanbu M, and Sakai T. Do cytokine-inducing substances penetrate through dialysis membranes and stimulate monocytes? *Kidney Int* 43 (Suppl 41): S205–208, 1993.
21. Morena M, Cristol JP, Senecal L, Leray-Moragues H, Krieter D, and Canaud B. Oxidative stress in hemodialysis patients: is NADPH oxidase complex the culprit? *Kidney Int* 80: 109–114, 2002.
22. Morena M, Delbosc S, Dupuy AM, Canaud B, and Cristol JP. Overproduction of reactive oxygen species in end-stage renal disease patients: a potential component of hemodialysis-associated inflammation. *Hemodial Int* 9: 37–46, 2005.
23. Morena M, Jaussent I, Chalabi L, Bargnoux AS, Dupuy AM, Badiou S, Rakic C, Thomas M, Canaud B, and Cristol JP. Biocompatibility of heparin-grafted hemodialysis membranes: impact on monocyte chemoattractant protein-1 circulating level and oxidative status. *Hemodial Int* 14: 403–410, 2010.
24. Niu XL, Madamanchi NR, Vendrov AE, Tchivilev I, Rojas M, Madamanchi C, Brandes RP, Krause KH, Humphries J, Smith A, Burnand KG, and Runge MS. Nox activator 1: a potential target for modulation of vascular reactive oxygen species in atherosclerotic arteries. *Circulation* 121: 549–559, 2010.
25. Niwa Y, Ozaki Y, Kanoh T, Akamatsu H, and Kurisaka M. Role of cytokines, tyrosine kinase, and protein kinase C on production of superoxide and induction of scavenging enzymes in human leukocytes. *Clin Immunol Immunopathol* 79: 303–313, 1996.
26. Pertosa G, Grandaliano G, Soccio M, Martino C, Gesualdo L, and Schena FP. Vitamin E-modified filters modulate Jun N-terminal kinase activation in peripheral blood mononuclear cells. *Kidney Int* 62: 602–610, 2002.
27. Pertosa G, Simone S, Soccio M, Marrone D, Gesualdo L, Schena FP, and Grandaliano G. Coagulation cascade activation causes CC chemokine receptor-2 gene expression and mononuclear cell activation in hemodialysis patients. *J Am Soc Nephrol* 16: 2477–2486, 2005.
28. Ray R and Shah AM. NADPH oxidase and endothelial cell function. *Clin Sci* 109: 217–226, 2005.
29. Sagedal S, Hartmann A, Sundstrøm K, Bjørnsen S, and Brosstad F. Anticoagulation intensity sufficient for haemodialysis does not prevent activation of coagulation and platelets. *Nephrol Dial Transplant* 16: 987–993, 2001.
30. Serfilippi G, Ferro T, and Johnson A. Activation of protein kinase C mediates altered pulmonary vasoreactivity induced by tumor necrosis factor-alpha. *Am J Physiol Lung Physiol* 267: L282–L290, 1994.
31. Sirolli V, Ballone E, Di Stante S, Amoroso L, and Bonomini M. Cell activation and cellular-cellular interactions during hemodialysis: effect of dialyzer membrane. *Int J Artif Organs* 25: 529–537, 2002.
32. Stenvinkel P, Carrero JJ, Axelsson J, Lindholm B, Heimbürger O, and Massy Z. Emerging biomarkers for evaluating cardiovascular risk in the chronic kidney disease patient: how do new pieces fit into the uremic puzzle? *Clin J Am Soc Nephrol* 3: 505–521, 2008.
33. Sumimoto H. Structure, regulation and evolution of Nox-family NADPH oxidases that produce reactive oxygen species. *FEBS J* 275: 3249–3277, 2008.
34. Vaziri ND, Dicus M, Ho ND, Boroujerdi-Rad L, and Sindhu RK. Oxidative stress and dysregulation of superoxide dismutase and NADPH oxidase in renal insufficiency. *Kidney Int* 63: 179–185, 2003.
35. Ward R and McLeish K. Hemodialysis with cellulose membranes primes the neutrophil oxidative burst. *Artif Organs* 19: 801–807, 1995.

Address correspondence to:
Dr. Giovanni Pertosa
Renal, Dialysis and Transplantation Unit
Department of Emergency and Organ Transplantation
University of Bari
Piazza Giulio Cesare, 11
70124 Bari
Italy

E-mail: g.pertosa@nephro.uniba.it

Date of first submission to ARS Central, May 9, 2011; date of final revised submission, November 4, 2011; date of acceptance, November 4, 2011.

Abbreviations Used

DCF-DA = 2′,7′-dichlorodihydrofluorescein diacetate
DPI = diphenyleneiodonium chloride
EVAL = ethylene-vinyl-alcohol
HBSS = Hanks' balanced salt solution
HD = hemodialysis
NAC = N-acetylcysteine
NADPH = nicotinamide adenine dinucleotide phosphate
PBMCs = peripheral blood mononuclear cells
PVDF = polyvinylidene fluoride
ROS = reactive oxygen species
SD = standard deviation
SEM = standard error of the mean
SOD = superoxide dismutase